ELSEVIER

Polymer 42 (2001) 4873–4884

polymer

www.elsevier.nl/locate/polymer

Monte Carlo simulation of tri-functional branching and tetra-functional crosslinking in emulsion polymerization of butadiene

E. Jabbari*

Laboratory of Biomaterials and Controlled Delivery Systems for Bioactive Agents, School of Biomedical Engineering, Amirkabir University of Technology, Tehran 15914, Iran

Received 20 June 2000; received in revised form 12 October 2000; accepted 4 December 2000

Abstract

A direct Monte Carlo method is used to simulate the effect of tri-functional long chain branching and tetra-functional crosslinking on molecular weight distribution in emulsion polymerization of butadiene. Butadiene polymerization, due to high extent of reaction with internal or pendant double bonds of polymer chains, can be used as a model to study the effect of tetra-functional crosslinking on polymer microstructure. In this simulation, elementary reactions included propagation, chain transfer to monomer, termination by disproportionation, transfer to C–H bond (BN3) and reaction with internal or pendant C=C bond (CL4) of growing and dead polymer chains. The initial polymerization volume of the simulation was 10^5 nm^3. The ratio of monomer to initiator concentration and initiator to polymer particles were 500 and 2.5, respectively, and the number of simulated polymer particles were 400. For simulated conversions in the range of 20–75% a bimodal molecular weight distribution was observed. The maximum of the second peak of the bimodal distribution moved to higher molecular weights as the conversion was increased. As the conversion was increased from 20 to 75%, the increase in the number average molecular weight of the polymer was linear but a slight increase in the slope of the weight average molecular weight was observed. More importantly, as the conversion was increased, a relatively sharp change in the slope of the weight fraction of the second peak of the molecular weight distribution curve was observed at approximately 20% conversion. According to the results, in polymerization systems with high extent of tetra-functional crosslinking, the development of the molecular weight distribution in emulsion polymerization is different from bulk systems. © 2001 Published by Elsevier Science Ltd.

Keywords: Simulation; Crosslinking; Butadiene

1. Introduction

Emulsion polymerization is used extensively in industry for production of high molecular weight polymers with fast reaction rates in submicron particulate form [1–3]. Considerable effort has been made to model and predict the structural properties of these polymers [4–6]. Harkins in 1945 [7] put forth a qualitative theory for emulsion polymerization in which he stated that polymer particles are formed by radicals entering the micelles. Smith and Ewart [8], based on Harkins theory, developed a model for emulsion polymerization in order to predict properties such as average particle size and molecular weight. Later, Min and Ray [9] proposed a comprehensive model for emulsion polymerization taking into account both homogeneous as well as micellar nucleation, radical desorption, particle coalescence and break-up.

In the past two decades, within the framework of Harkins theory, efforts have been made to model and simulate the microstructure of polymeric chains produced by emulsion polymerization such as molecular weight distribution, extent of branching, effect of termination mode, and crosslinking [10–16]. Lichti et al. [13,14] presented a mathematical formulation to describe the evolution of the molecular weight distribution (MWD) of linear chains in emulsion polymerization. Min and Ray [9,11] developed a comprehensive mathematical model consisting of complex population balance equations to predict MWD, branching and crosslinking. However, due to complexity of the resulting partial differential equations only moments of the distribution could be determined successfully. Sundberg and Eliason [17] developed a mathematical model for the calculation of MWD in emulsion polymerization with only zero or one radical per particle. Friis and Hamielec [18] derived equations for the MWD in emulsion polymerization under zero or one condition with chain transfer to monomer and polymer. Giannetti et al. [15] used a probabilistic approach to describe the MWD in emulsion polymerization with zero,

* Tel./fax: +98-1-649-5655.
E-mail address: ejabari@cic.aku.ac.ir (E. Jabbari).

0032-3861/01/$ - see front matter © 2001 Published by Elsevier Science Ltd.
PII: S0032-3861(00)00880-6

Nomenclature

f	Initiator efficiency
I	Initiator
[I]	Initiator concentration in the aqueous phase, mol cm^{-3}
K_d	Initiator dissociation constant, s^{-1}
K_p	Propagation rate constant, l mol^{-1} s^{-1}
K_{td}	Termination by disproportionation rate constant, l mol^{-1} s^{-1}
K_{tm}	Transfer to monomer rate constant, l mol^{-1} s^{-1}
K_{ta}	Transfer to agent rate constant, l mol^{-1} s^{-1}
K_{tph}	Rate constant for transfer to the C–H bond of polymer, l mol^{-1} s^{-1}
K_{tfc}	Rate constant for transfer to the C=C bond of polymer, l mol^{-1} s^{-1}
m_{pi}	Number of monomers in the ith particle
M	Monomer
[M_{pi}]	Monomer concentration in the ith particle, mol cm^{-3}
[MP_{pi}]	Concentration of polymerized monomers in the ith particle, mol cm^{-3}
N_{av}	Avogadro number
$P(j)$	Selection probability for the jth particle
P_{diss}	Probability of dissociation
$P_{gri}(l)$	Selection probability for the growing radical l in the ith particle
P_n	Polymer chain with n repeat units
$P_{pcdi}(l)$	Probability for transfer to the C=C bond of polymer chain l in ith particle
$P_{pchi}(l)$	Probability for transfer to the C–H bond of polymer chain l in the ith particle
P_{pi}	Probability for propagation in the ith particle
P_{tai}	Probability for transfer to agent in the ith particle
P_{tdi}	Probability for termination in the ith particle
P_{tmi}	Probability of transfer to monomer in the ith particle
P_{tfci}	Probability for transfer to the C=C bond of polymer in the ith particle
P_{tphi}	Probability for transfer to the C–H bond of polymer in the ith particle
[PP]	Concentration of polymer particles, mol cm^{-3}
PR$^{\cdot}$	Primary radical
r_{pi}	Number of growing radicals in the ith particle
R_i	Rate of initiation, mol l^{-1} s^{-1}
R$^{\cdot}_n$	Growing radical with n repeat units
R_{pi}	Rate of propagation in the ith particle, mol l^{-1} s^{-1}
R_{tai}	Rate of transfer to agent in the ith particle, mol l^{-1} s^{-1}
R_{tdi}	Rate of termination in the ith particle, mol l^{-1} s^{-1}
R_{tmi}	Rate of transfer to monomer in the ith particle, mol l^{-1} s^{-1}
R_{toti}	Total rate of reaction in the ith particle, mol l^{-1} s^{-1}
R_{tfci}	Rate of transfer to the C=C bond of polymer in ith particle, mol l^{-1} s^{-1}
R_{tphi}	Rate of transfer to the C–H bond of polymer in ith particle, mol l^{-1} s^{-1}
[$R^{\cdot}_{pi}$]	Concentration of growing radical in the ith particle, mol cm^{-3}
$t_{1/2}$	Half life of initiator, s
T	Temperature, °C
TA	Transfer agent
TA$^{\cdot}$	Transfer agent radical
[T_{pi}]	Concentration of transfer agent in the ith particle, mol cm^{-3}
V_{aq}	Volume of the aqueous phase, cm^3
V_{pi}	Volume of the ith particle, cm^3
V_{sim}	Initial volume of the simulated polymerization system, nm^3
Δt_i	Time interval, s
δt_{init}	Elapsed time for initiation per molecule, s
δt_{pi}	Elapsed time for propagation per molecule, s
δt_{tai}	Elapsed time for transfer to agent per molecule, s
δt_{tdi}	Elapsed time for termination per molecule, s
δt_{tmi}	Elapsed time for transfer to monomer per molecule, s
δt_{tfci}	Elapsed time for transfer to the C=C bond of polymer per molecule, s
δt_{tphi}	Elapsed time for transfer to the C–H bond of polymer per molecule, s
ρ_B	Density of butadiene, g cm^{-3}
ρ_{PB}	Density of polybutadiene, g cm^{-3}

one or two radicals per particle. None of these models can properly predict microstructural features of chains such as extent of branching, microgel formation, crosslinking and the distribution of molecular weight in emulsion polymerization.

The method of moments [19–31] has been applied successfully to calculate average molecular weights in free radical polymerization with long chain branching and crosslinking based on the assumption that no more than one radical center per polymer radical is permissible. Method of moments provides information on the various molecular weights but modality and chain length distribution cannot be predicted except for very simple cases. Also, a crosslinked gel molecule is a polymer molecule with many radical centers [32]. These polyradicals can have significant effect on MWD especially in emulsion polymerization where very long molecules are produced.

Recently, a new theory for non-linear polymerization that includes branching and crosslinking has been proposed [33–40]. This theory is based on the branching density

distribution (BDD) formed in a non-equilibrium system which can give exact solutions for the statistical properties of non-linear polymer molecules. In emulsion polymerization, polymer particles contain between 100 and 1000 polymer molecules which cannot be considered infinite whereas the BDD method assumes infinite number of polymer chains [34]. As previously stated [41], if the frequency of branching is not very large, a simulation method based on BDD can be used to describe the kinetics of non-linear emulsion polymerization. However, as the branching density increases, the fact that each polymer particle consists of a limited number of polymer molecules necessitates a model that accounts for the compartmentalization effect in emulsion polymerization.

Tobita and Yamamoto [42] have studied the formation of bimodal molecular weight distribution in emulsion crosslinking coploymerization of vinyl and divinyl monomers using the method of Monte Carlo simulation. According to their simulation results, in emulsion polymerization bimodal distributions are formed due to the limited reaction space within the polymer particle. This means that large polymer molecules belonging to the high molecular weight peak want to grow further but they cannot grow due to the limitation of a small particle size. Tobia [43] has also studied the formation of bimodal distribution in bulk polymerization systems. According to his results, the formation of bimodal distribution in bulk systems depends on size and structure of the crosslinking reaction. Therefore, according to these simulation results, the process of formation of bimodal distribution in emulsion polymerization is quite different from the process for bulk systems. The emulsion polymerization system gives a size dependence because crosslinking between large-sized polymer molecules that exist in different polymer particles are prohibited. Moreover, Tobita and Yamamoto [42] simulated the kinetics of microgel formation in emulsion copolymerization of vinyl and divinyl monomers. They observed that a drastic increase in molecular weight at the gel point that is a characteristic of homogeneous polymerization is not a requisite for microgel formation and a new definition for gel point may be required in emulsion polymerization. According to their simulation results the formation of microgel, defined as intramolecularly crosslinked macromolecules with sufficiently high molecular weight, depends strongly on reaction parameters such as the feed ratio and reactivity ratio of the vinyl and divinyl monomers and ratio of the rate constant for the crosslinking reaction to the propagation reaction. They further observed that, in some cases depending on reaction parameters, very large polymer molecules that contain many intermolecular crosslinks are formed without the formation of intramolecular crosslinks.

The objective of this research was to investigate the effect of tri-functional long chain branching and tetra-functional crosslinking on chain length distribution and microgel formation in emulsion polymerization of dienes. In this system, tri-functional branching and tetra-functional crosslinking are caused by radical transfer to C–H bond and reaction with internal or pendant C=C bond of the polymerized butadiene monomers, respectively. At present, none of the theoretical models can adequately describe these effects in emulsion polymerization of diene monomers with high degree of branching and crosslinking. Therefore, a direct Monte Carlo simulation method was used in this work to study the effect of tri-functional branching and tetra-functional crosslinking on chain length distribution. Emulsion polymerization of butadiene was used as a model system to study these effects.

2. Theory and simulation

2.1. Elementary reactions

Due to complexity of the moment method in systems with tetra-functional crosslinking and because of the limitations of the BDD method for systems with small particle size, direct Monte Carlo simulation was used. The following elementary reactions were used in the simulation:

$$\mathrm{I} \xrightarrow{f,K_d} 2\mathrm{PR}^{\cdot} \tag{1}$$

$$\mathrm{PR}^{*} + \mathrm{M} \xrightarrow{K_p} \mathrm{R}_1^{\cdot} \tag{2}$$

$$\mathrm{R}_n^{\cdot} + \mathrm{M} \xrightarrow{K_p} \mathrm{R}_{n+1}^{\cdot} \tag{3}$$

$$\mathrm{R}_n^{\cdot} + \mathrm{R}_m^{\cdot} \xrightarrow{K_{td}} \mathrm{P}_n + \mathrm{P}_m \tag{4}$$

$$\mathrm{R}_n^{\cdot} + \mathrm{M} \xrightarrow{K_{tm}} \mathrm{P}_n + \mathrm{R}_1^{\cdot} \tag{5}$$

$$\mathrm{R}_n^{\cdot} + \mathrm{TA} \xrightarrow{K_{ta}} \mathrm{P}_n + \mathrm{TA}^{\cdot} \tag{6}$$

$$\mathrm{R}_n^{\cdot} + \mathrm{P}_m \xrightarrow{K_{tph}} \mathrm{P}_n + \mathrm{R}_m^{\cdot} \tag{7}$$

$$\mathrm{R}_n^{\cdot} + \mathrm{P}_m \xrightarrow{K_{tfc}} \mathrm{R}_{n+m}^{\cdot} \tag{8}$$

In the above reactions, I, $\mathrm{PR}^{\cdot}$, M, $\mathrm{R}_1^{\cdot}$, TA, and $\mathrm{TA}^{\cdot}$ represent initiator, primary radical, monomer, growing radical with one repeat unit, transfer agent, and transfer agent radical, respectively. Symbols R_n and P_n represent growing polymer radical and dead polymer chain with n number of repeat units, respectively. Rate constants K_d, K_p and K_{td} are for dissociation, propagation, and termination by disproportionation, respectively. Rate constants K_{tm}, K_{ta}, K_{tph} and K_{tfc} are for transfer to monomer, chain transfer agent, transfer to the C–H bond and reaction of the growing radical with internal or pendant double bond of butadiene chains, respectively.

Reactions (1) and (2) occur exclusively in the aqueous phase and reactions (2)–(8) happen exclusively in the polymer particle phase. In reaction (1), an initiator molecule

dissociates thermally in the aqueous phase to produce two primary radicals. In reaction (2), the primary radical reacts with a butadiene monomer, becoming insoluble in the aqueous phase, and is absorbed by the polymer particles. In reaction (3), propagation step takes place in the polymer particle by the reaction of a growing radical with a monomer. After a monomer reacts, its equilibrium concentration in the polymer particle is recalculated using the Flory–Huggins theory, assuming homogeneous particle morphology, and based on the new concentration, the reacted monomer is replaced from the monomer particles.

In reaction (4), termination occurs by the reaction of two growing radicals in the polymer particle phase. For butadiene, termination takes place mainly by disproportionation with the formation of two dead polymer chains and a double bond at the end of one chain. Reaction of the growing radical with this double bond was also taken into account in this simulation. In reaction (5), a growing radical transfers its radical to a monomer resulting in a dead polymer chain with a double bond at the terminated end and a monomer radical. This monomer radical is able to grow by propagation. Reaction of the growing radical with the double bond of the polymer chain formed by reaction (5) was accounted for in this simulation. Reaction (6) is similar to reaction (5) except that a chain transfer agent is used in place of monomer. It is assumed that the chain transfer agent radical, $TA^{\cdot}$, is inactive and cannot grow by propagation.

In reaction (7), a growing radical reacts with one of the C–H bonds on a dead polymer chain, extracts a hydrogen from the C–H bond, and becomes a dead polymer chain with no double bond at the terminated end. The reacted polymer chain, after loosing a hydrogen, becomes a growing polymer radical with a new branch to grow from the site of hydrogen abstraction. In the simulation, chain transfer to the C–H bond of dead polymer chains as well as growing polymer radicals was allowed, although the extent of branching by chain transfer to growing radicals was relatively low. In reaction (8), a growing radical with n units reacts with one of the internal or pendant C=C bonds on a dead polymer chain with m units, forming a new polymeric radical with $(m + n)$ units. Since two polymeric chains are connected by reaction (8), this reaction causes crosslinking and, in some cases, microgel formation in emulsion polymerization.

2.2. Simulation assumptions

1. A polymer particle is formed by a primary radical entering a micelle and polymerization continued only within the polymer particle. Since the solubility of butadiene monomer in the aqueous phase was only 0.018% at 25°C, therefore polymerization in the continuous phase and homogeneous nucleation were not significant.
2. All of the polymer particles were formed simultaneously at zero conversion. Distribution of birth time of particles affects mainly the particle size distribution and not the microstructure of polymer chains. Therefore, the number of polymer particles was constant during the course of this simulation.
3. Initiator molecules dissociated in the aqueous continuous phase, forming two primary radicals. Then, these primary radicals, after reacting with a monomer in the aqueous phase, became insoluble due to very low solubility of butadiene in water and they were adsorbed by the polymer particles. Propagation occurred exclusively in the polymer particles.
4. Radical desorption from the polymer particles to the aqueous phase was not significant. This assumption allowed us to focus on the effect of tri-functional branching and tetra-functional crosslinking on MWD irrespective of radical desorption.
5. Particle coalescence was not significant. Particle coalescence mainly affects particle size distribution and not the microstructure of polymer chains.
6. Polymer particles were homogeneous and the concentration of monomer within the particles was determined by the Flory–Huggins equation.
7. The effect of surface free energy on equilibrium concentration of each component within a particle was ignored. This effect became important for particles smaller than 50 nm in diameter.
8. Elementary reactions were not diffusion controlled. So, the reaction rate constants for propagation, chain transfer, crosslinking, and termination were assumed constant during the course of the simulation. Since the glass transition temperature of butadiene is well below ambient temperature and the extent of reaction was never more than 75%, this was a good assumption.
9. Particles were saturated with monomer and monomer particles were present throughout the course of the polymerization.
10. Polymerization reaction was carried out batchwise but the reaction volume could change during the course of the reaction.
11. For a given conversion, all of the C–H or C=C groups of the polymer chains for tri-functional branching and tetra-functional crosslinking were equally reactive. Therefore, the effect of steric hindrance or excluded volume on reactivity was not considered in this simulation.
12. Cyclization was equally probable for all of the reacting C–H and C=C groups on a polymer chain. Therefore, the effect of chain length on reactivity and cyclization was not considered in this simulation [44].

Monte Carlo method can easily simulate polymerization reactions without being limited by the above assumptions. However, the above assumptions helped us to focus on the effect of tri-functional branching and tetra-functional crosslinking on the microstructure of polymer chains and microgel formation without interference from other reaction conditions.

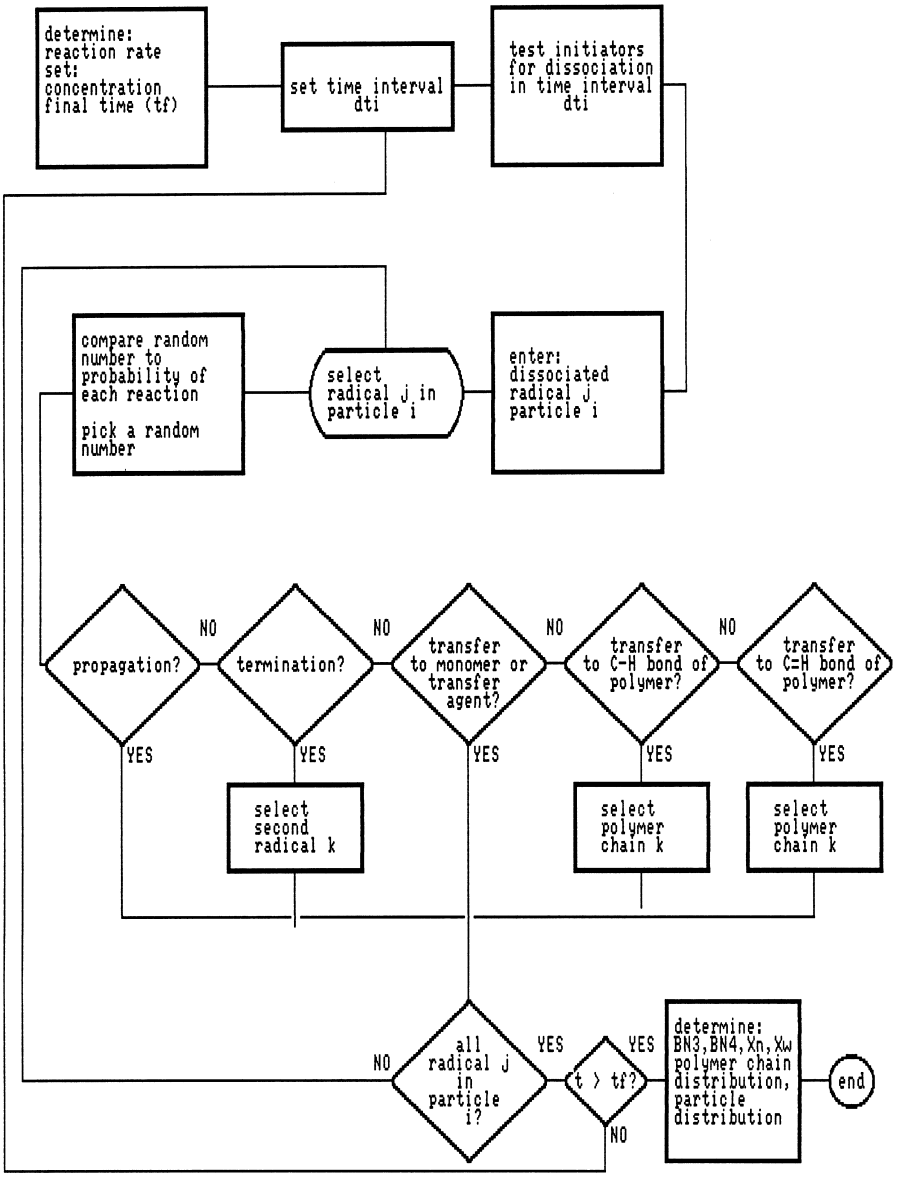

Fig. 1. Simulation algorithm for emulsion polymerization of butadiene.

2.3. Simulation procedure

The simulation algorithm is presented in Fig. 1. To begin the simulation, the number of polymer particles, number of monomer and initiator molecules, initiator half-life and the rate constants for each reaction were determined. A subroutine was developed for generation of random numbers between zero and one. This subroutine was tested for variance and for correlation between neighboring numbers for at least one billion numbers. The variance was within the standard limits and no correlation was found between the neighboring numbers.

2.3.1. Initiation in the aqueous phase

Each initiator molecule was dissociated directly by random number generation. A time interval, Δt_i, much shorter than the half-life of initiator was selected. Then, probability of dissociation of a particular initiator molecule, P_{diss}, was determined by:

$$P_{\text{diss}} = K_{\text{d}}\Delta t_i = [\ln 2/t_{1/2}]\Delta t_{\text{i}} \tag{9}$$

In the above equation, $t_{1/2}$ is the initiator half-life. For each initiator molecule a random number, RANDOM, was picked by the random number generator subroutine. If $0 \leq \text{RANDOM} \leq P_{\text{diss}}$, then the molecule was dissociated and two primary radicals were produced. On the other hand, if $P_{\text{diss}} < \text{RANDOM} \leq 1$, then the molecule was left undissociated. This process was repeated for each initiator molecule that was not dissociated in the previous time interval Δt_{i-1}. The time elapsed for a initiator to dissociate was

determined by:

$$\delta t_{\text{init}} = 1/[R_i V_{aq} N_{av}] \quad (10)$$

In the above equation R_i and N_{av} are the initiation rate and Avogadro number, respectively. V_{aq} is the volume of the aqueous phase. The primary radicals produced in the continuous phase initiated polymerization in the particle phase. The primary radical produced in the aqueous phase entered a polymer particle based directly on random number generation. A selection probability was assigned to each polymer particle based on its surface area. It was assumed that initially at time zero polymer particles were micelles with diameter of 2 nm. As the reaction proceeded, a distribution of particle sizes developed. A random number was generated and a radical produced in the aqueous phase was allowed to enter the *i*th particle if the following criteria was satisfied:

$$\sum_{j=1}^{i-1} P(j) \le \text{RANDOM} < \sum_{j=1}^{i} P(j) \quad (11)$$

In the above criteria, *j* is the particle number ranging from 1 to *n*, $P(j)$ is the selection probability of the *j*th particle.

2.3.2. Reactions within the particle phase

After a radical entered a particle, polymerization proceeded by propagation, transfer to monomer, to transfer agent, transfer to the C–H bonds of the polymer, crosslinking with the internal or pendant C=C bonds of the polymer or termination by disproportionation, with predetermined probabilities. The rate of the above reactions are given by:

$$R_{pi} = K_p[M_{pi}][R^{\cdot}_{pi}] \quad (12)$$

$$R_{tdi} = K_{td}[R^{\cdot}_{pi}][R^{\cdot}_{pi}] \quad (13)$$

$$R_{tmi} = K_{tm}[M_{pi}][R^{\cdot}_{pi}] \quad (14)$$

$$R_{tai} = K_{ta}[T_{pi}][R^{\cdot}_{pi}] \quad (15)$$

$$R_{tphi} = K_{tph}[R^{\cdot}_{ppi}][M_{ppi}] \quad (16)$$

$$R_{tfci} = K_{tfc}[R^{\cdot}_{pi}][M_{ppi}] \quad (17)$$

In the above equations, R_{pi}, R_{tdi}, R_{tmi}, R_{tai}, R_{tphi} and R_{tfci} are the rate of propagation, rate of termination by disproportionation, rate of transfer to monomer, to transfer agent, transfer to the C–H bond, reaction with the C=C bond of the polymer chains, respectively, for the *i*th particle. $[M_{pi}]$, $[R^{\cdot}_{pi}]$, $[T_{pi}]$ and $[MP_{pi}]$ are the concentrations of monomer, radical, transfer agent and polymerized monomers for the *i*th particle, respectively. The concentration of monomer and radical in the *i*th particle was determined by:

$$[M_{pi}] = m_{pi}/[N_{av} V_{pi}] \quad (18)$$

$$[R^{\cdot}_{pi}] = r_{pi}/[N_{av} V_{pi}] \quad (19)$$

In the above equations, m_{pi} and r_{pi} are the number of molecules of monomer and radicals in the *i*th particle, respectively, and V_{pi} is the volume of the *i*th particle. The concentrations $[T_{pi}]$ and $[MP_{pi}]$ were determined in a similar manner.

The state space for the simulation included all of the elementary reactions (12)–(17). An event in the simulation was defined as the occurrence of one of the reactions in the state space for the *j*th radical in the *i*th particle. The selection probability of each reaction in the state space was assumed to be proportional to the rate of the corresponding reaction, as given below:

$$P_{pi} = R_{pi}/R_{toti} \quad (20)$$

$$P_{tdi} = R_{tdi}/R_{toti} \quad (21)$$

$$P_{tmi} = R_{tmi}/R_{toti} \quad (22)$$

$$P_{tai} = R_{tai}/R_{toti} \quad (23)$$

$$P_{tphi} = R_{tphi}/R_{toti} \quad (24)$$

$$P_{tfci} = R_{tfci}/R_{toti} \quad (25)$$

where

$$R_{toti} = R_{pi} + R_{tdi} + R_{tmi} + R_{tai} + R_{tphi} + R_{tfci} \quad (26)$$

In the above equations, P_{pi}, P_{tdi}, P_{tmi}, P_{tai}, P_{tphi} and P_{tpdi} are the selection probability for propagation, termination by disproportionation, transfer to monomer, to transfer agent, transfer to the C–H bonds and reaction with the C=C bonds of the polymer, respectively, for the *i*th particle. These probabilities also depended on reaction time as the concentrations of each component changed with time.

2.3.2.1. Propagation. A random number, RANDOM, was picked by the random number generator subroutine. If $0 \le \text{RANDOM} \le P_{pi}$, then the event propagation was selected for the *j*th growing radical in the *i*th particle and a monomer was added to the growing radical *j*. After each event, the new concentration of monomer was determined from the Flory–Huggins equation. To reach the new concentration, monomer was added to the *i*th particle from the monomer droplets. The time elapsed for the propagation event to occur, δt_{pi}, in the *i*th particle with volume V_i was determined by:

$$\delta t_{pi} = 1/[R_{pi} V_{pi} N_{av}] \quad (27)$$

2.3.2.2. Termination. A random number was picked and if $P_{pi} < \text{RANDOM} \le P_{pi} + P_{tdi}$, then the event termination was selected for the *j*th growing radical in the *i*th particle. Termination required simultaneous cessation of two growing radicals *j* and *k*. To choose the growing radical *k*, a selection probability was assigned to each growing radical in the *i*th particle based on its number of monomer units. A

random number was generated and the growing radical k in the ith particle was selected if the following criteria was satisfied:

$$\sum_{l=1}^{k-1} P_{\mathrm{gr}i}(l) \le \mathrm{RANDOM} < \sum_{l=1}^{k} P_{\mathrm{gr}i}(l) \tag{28}$$

In the above criteria, l is the growing radical number and $P_{\mathrm{gr}i}(l)$ is the selection probability for the growing radical number l in the ith particle. After the kth radical was selected, it was terminated simultaneously with the jth radical with the production of two polymer chains with degree of polymerization equal to the number of repeat units on their respective radicals and a double bond at the end of one of these chains. This double bond was also taken into account in the crosslinking reaction with the C=C bond of the polymer chains. The time elapsed for the termination event to occur, $\delta t_{\mathrm{td}i}$, in the ith particle was determined by:

$$\delta t_{\mathrm{td}i} = 1/[R_{\mathrm{td}i} V_i N_{\mathrm{av}}] \tag{29}$$

2.3.2.3. Chain transfer to monomer and transfer agent. A random number, RANDOM, was picked. If $P_{\mathrm{p}i} + P_{\mathrm{td}i} < \mathrm{RANDOM} \le P_{\mathrm{p}i} + P_{\mathrm{td}i} + P_{\mathrm{tm}i}$, then the event transfer to monomer was selected for the jth growing radical in the ith particle. If $P_{\mathrm{p}i} + P_{\mathrm{td}i} + P_{\mathrm{tm}i} < \mathrm{RANDOM} \le P_{\mathrm{p}i} + P_{\mathrm{td}i} + P_{\mathrm{tm}i} + P_{\mathrm{ta}i}$, then the event transfer to transfer agent was selected for the jth growing radical in the ith particle. Transfer to monomer resulted in the production of a polymer chain and a new growing radical with one monomer unit, $R_1^{\cdot}$. Transfer to transfer agent resulted in the production of a polymer chain and an inactive primary radical, $TA^{\cdot}$. The time elapsed for the event transfer to monomer, $\delta t_{\mathrm{tm}i}$, and to transfer agent, $\delta t_{\mathrm{ta}i}$, to occur in the ith particle were determined by:

$$\delta t_{\mathrm{tm}i} = 1/[R_{\mathrm{tm}i} V_i N_{\mathrm{av}}] \tag{30}$$

$$\delta t_{\mathrm{ta}i} = 1/[R_{\mathrm{ta}i} V_i N_{\mathrm{av}}] \tag{31}$$

2.3.2.4. Tri-functional branching (BN3). A random number, RANDOM, was picked. If the following criteria was satisfied, then the event transfer to the C–H bond of the polymer chains was selected for the jth growing radical in the ith particle:

$$P_{\mathrm{p}i} + P_{\mathrm{td}i} + P_{\mathrm{tm}i} + P_{\mathrm{ta}i} < \mathrm{RANDOM} \le P_{\mathrm{p}i} + P_{\mathrm{td}i} + P_{\mathrm{tm}i} + P_{\mathrm{ta}i} + P_{\mathrm{tph}i} \tag{32}$$

Transfer to the C–H bond resulted in the production of a side chain on a polymer chain. To choose the polymer chain k for radical transfer, a selection probability was assigned to each polymer chain in the ith particle based on its number of H–C–H units. A random number was generated and the polymer chain l in the ith particle was selected if the following criteria was satisfied:

$$\sum_{l=1}^{k-1} P_{\mathrm{pch}i}(l) \le \mathrm{RANDOM} < \sum_{l=1}^{k} P_{\mathrm{pch}i}(l) \tag{33}$$

In the above criteria, l is the polymer chain number and $P_{\mathrm{pch}i}(l)$ is the selection probability for the polymer chain number l in the ith particle. After the kth polymer was selected, the number of branches on this polymer chain was increased by one and this chain was allowed to propagate from the branch point in the next events. The time elapsed for tri-functional branching event to occur, $\delta t_{\mathrm{tph}i}$, in the ith particle was determined by:

$$\delta t_{\mathrm{tph}i} = 1/[R_{\mathrm{tph}i} V_i N_{\mathrm{av}}] \tag{34}$$

2.3.2.5. Tetra-functional crosslinking (CL4). A random number, RANDOM, was picked. If the following criteria was satisfied, then the event transfer to the C=C bond of the polymer chains was selected for the jth growing radical in the ith particle:

$$P_{\mathrm{p}i} + P_{\mathrm{td}i} + P_{\mathrm{tm}i} + P_{\mathrm{ta}i} + P_{\mathrm{tph}i} < \mathrm{RANDOM} \le P_{\mathrm{p}i} + P_{\mathrm{td}i} + P_{\mathrm{tm}i} + P_{\mathrm{ta}i} + P_{\mathrm{tph}i} + P_{\mathrm{tfc}i} \tag{35}$$

Reaction with the C=C bond resulted in the production of a crosslink point between a growing radical and a polymer chain. To choose the polymer chain k for crosslinking, a selection probability was assigned to each polymer chain in the ith particle based on its number of C=C bonds. A random number was generated and the polymer chain l in the ith particle was selected if the following criteria was satisfied:

$$\sum_{l=1}^{k-1} P_{\mathrm{pcd}i}(l) \le \mathrm{RANDOM} < \sum_{l=1}^{k} P_{\mathrm{pcd}i}(l) \tag{36}$$

In the above criteria, l is the polymer chain number and $P_{\mathrm{pcd}i}(l)$ is the selection probability for the polymer chain number l in the ith particle. After the kth polymer was selected, a new growing radical z with $(m + n)$ repeat units was produced, with m and n being the number of repeat units of the kth polymer chain and jth growing radical before the reaction, respectively. This new growing radical was allowed to propagate further from the crosslink point in the next events. The time elapsed for tetra-functional crosslinking event to occur, $\delta t_{\mathrm{tfc}i}$, in the ith particle was determined by:

$$\delta t_{\mathrm{tfc}i} = 1/[R_{\mathrm{tfc}i} V_i N_{\mathrm{av}}] \tag{37}$$

The above process was repeated for each growing radical in the ith particle and for all of the particles that contained growing radicals. After each event, the total time elapsed was determined. If the elapsed time was greater than or equal to the specified time, t_i, then a new time interval Δt_i was selected and the whole process of initiation and reactions within the particles for each new growing radical

Table 1
Physico-chemical properties for emulsion polymerization of butadiene

K_p (l mol^{-1} s^{-1})	18
K_{td} (l mol^{-1} s^{-1})	15×10^{7}
K_{tm} (l mol^{-1} s^{-1})	3.1×10^{-3}
K_{tph} (l mol^{-1} s^{-1})	2×10^{-2}
K_{tpd} (l mol^{-1} s^{-1})	18
ρ_B (g/cm^3)	0.62
ρ_{PB} (g/cm^3)	0.96
$t_{1/2}$ (s)	1800
V_{sim} (nm^3)	10^5
[M]/[I]	500
[I]/[PP]	2.5
No. of polymer particles	400
T (°C)	25

produced in the aqueous phase was repeated. When the total elapsed time was greater or equal to the final time of the reaction, t_f, the simulation was stopped.

Physical properties such as chain length distribution, number and weight average chain length, number of transfers to monomer and microstructural features such as extent of tri-functional branching (BN3) and tetra-functional crosslinking (CL4) was determined from the simulation results for each polymer particle or for the collection of particles in the simulated emulsion polymerization system. Rate constants, concentrations, and other properties for the simulated polymerization reaction are given in Table 1. For K_p, a value of 100 l mol^{-1} s^{-1} at 60°C is reported for butadiene in Ref. [45] with activation energy of 9.3 kCal mol^{-1} and activation constant of 1.2×10^{8} l mol^{-1} s^{-1}. Using the Arrhenius equation, a value of 18 l mol^{-1} s^{-1} is obtained for K_p at 25°C. Ref. [46] reports the same value for K_p of butadiene at 60°C. The polymer handbook [47] reports the value of 8.4 lit mol^{-1} s^{-1} for K_p of butadiene at 10°C, but no values of activation energy and activation constant are reported. When the K_p value from Ref. [45] is extrapolated to 10°C using the Arrhenius equation, a value of 7.9 l mol^{-1} s^{-1} is obtained which is close to the K_p in the polymer handbook. Therefore, the value of 18 l mol^{-1} s^{-1} was used for K_p of butadiene at 25°C in the simulation.

For K_{td} of butadiene, no value is reported in the polymer handbook [47]. Therefore, it was approximated using the K_t values of other polymerization systems. In butadiene the terminal carbon atom, to which the growing radical is attached, has either H and CH=CH$_2$ groups or two H groups. If the terminal carbon atom has H and CH=CH$_2$ groups, it has some resemblance to the terminal carbon atom in polystyrene with H and phenyl ring but with one instead of three conjugated double bonds. If the terminal carbon atom has two H groups, it resembles the terminal carbon in polyethylene. The butadiene radical is less sterically hindered compared to polystyrene but more sterically hindered compared to polyethylene. Also, the butadiene radical is relatively more stable than polyethylene but less stable than polystyrene radical. Therefore, on the basis of steric hindrance and radical stability, the K_t of butadiene radical should be between the K_t of polystyrene and polyethylene radicals. Therefore, in the absence any data, the K_t of butadiene was approximated by the K_t values of ethylene and styrene. Ref. [46] reports the values of 6×10^{7} and 54×10^{7} l mol^{-1} s^{-1} at 60°C for K_t of styrene and ethylene with activation energies of 8 and 1.3 kJ mol^{-1}, respectively. Using the Arrhenius equation, the values of 4.3×10^{7} and 51×10^{7} l mol^{-1} s^{-1} was obtained at 25° for styrene and ethylene, respectively. Then, a geometric mean was used to approximate the K_t of butadiene from the K_t values of ethylene and styrene. Using a geometric mean, the value of 15×10^{7} l mol^{-1} s^{-1} was obtained for butadiene at 25°C and this value was used in the simulation.

No K_{tm} value is reported for free radical polymerization of butadiene in the polymer handbook. Since the chemical structures of butadiene and 1-butene are relatively close, the chain transfer constant to monomer, C_m, of butadiene was approximated by the C_m of 1-butene. According to the polymer handbook [47], the C_m of 1-butene at 40, 50 and 60°C are 3.1×10^{-4}, 5.1×10^{-4} and 7.3×10^{-4}, respectively. Also, using the K_p value from Ref. 45 and the Arrhenius equation, the K_p of butadiene at 40, 50 and 60°C are 40, 60 and 100 l mol^{-1} s^{-1}, respectively. Therefore, the K_{tm} of butadiene at 40, 50 and 60°C are 124×10^{-4}, 306×10^{-4} and 730×10^{-4} l mol^{-1} s^{-1}, respectively. With these K_{tm} values and using the Arrhenius equation, the value of 3.1×10^{-3} l mol^{-1} s^{-1} was obtained for K_{tm} of butadiene at 25°C and this value was used in the simulation. No chain transfer agent, TA, was used in this simulation.

The polymer handbook [47] reports the value of 11×10^{-4} for chain transfer constant to polymer for butadiene at 50°C. It was assumed that this value is due to chain transfer to the C–H bond of polybutadiene chains and did not include tetra-functional crosslinking. In the absence of data at other temperatures, this value was used as C_{tph} for butadiene at 25°C. Since the K_p of butadiene at 25°C was equal to 18 l mol^{-1} s^{-1}, the value of 2×10^{-2} l mol^{-1} s^{-1} was obtained for K_{tph} and this value was used in the simulation. For estimation of K_{tfc}, the structure and chain length dependence of the reactivity of the pendant or internal double bond of the polymer chains were neglected. Therefore, the space dimensionality was not included in this simulation and it was also assumed that the reaction of a growing radical with a pendant or internal double bond was not diffusion controlled. Therefore, the value of K_{tfc} was assumed to be equal to the value of K_p for butadiene. The value of 18 l mol^{-1} s^{-1} was used for K_{tfc} at 25°C in this simulation.

For density of butadiene monomer and polybutadiene, the values of 0.62 and 0.96 g cm^{-3}, respectively, at 25°C were obtained from Ref. [48]. The half-life of the initiator, $t_{1/2}$, was 1800 s, the volume of the simulation was 10^5 nm^3, the ratio of monomer to initiator concentration was 500, the ratio of initiator to polymer particle concentration was 2.5, the temperature was 25°C. As the number of particles increased to more than 400, no significant change in the

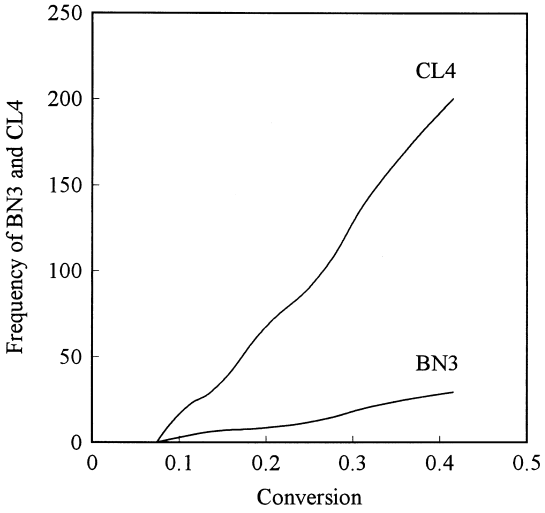

Fig. 2. Simulated frequency of tri-functional branching and tetra-functional crosslinking as a function of conversion for emulsion polymerization of butadiene at 25°C.

chain length distribution for all of the particles was observed. Therefore, all simulations were performed with 400 polymer particles. The run time of the simulation on a 300 MHz personal computer was approximately 2 h.

3. Results and discussion

Fig. 2 shows the frequency of tri-functional branching and tetra-functional crosslinking in emulsion polymerization of butadiene. According to this figure, frequency of BN3 branching and CL4 crosslinking increased linearly with conversion and the rate of BN4 was at least an order of magnitude higher than BN3. According to Friedman [49], the best way to distinguish between a unimodal and bimodal distribution is to plot weight fraction of the logarithm (base 10) of chain length, $W[\log(n)]$, versus logarithm of chain length, $\log(n)$. Therefore, the chain length distributions are

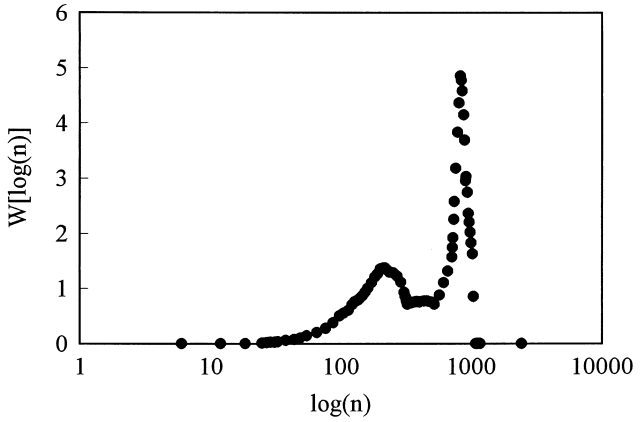

Fig. 4. Simulated weight fraction of logarithm of chain length, $W[\log(n)]$, versus $\log(n)$ at 40% conversion for emulsion polymerization of butadiene at 25°C.

presented in Figs. 3–6 as $W[\log(n)]$ versus $\log(n)$ for the simulated system at 20, 40, 55and 75% conversion, respectively. For 20% conversion, a short second peak with maximum chain length of 450 attached to a larger first peak is observed. This indicates that the chain length distribution was bimodal for 20% conversion. As the conversion was increased to 40%, the second peak became completely separate from the first peak with a maximum chain length of 800 repeat units. With increasing conversion to 55 and 75%, this maximum increased to 1200 and 1950 repeat units, respectively. Also, as the conversion was increased, the fraction of the second peak increased significantly. As the conversion was increased from 20 to 40 to 55 and 75%, the number fraction of the second peak of the distribution increased approximately in a linear fashion from zero to 0.2 to 0.41 and 0.6, respectively, and the weight fraction of the second peak increased in a non-linear fashion from 0.11 to 0.48 to 0.73 and 0.94, respectively. In the absence of tetra-functional crosslinking, only a tail was observed on the high side of the chain length distribution for all conversions

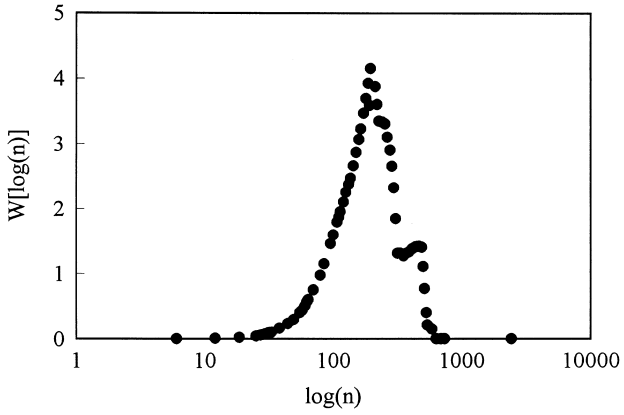

Fig. 3. Simulated weight fraction of logarithm of chain length, $W[\log(n)]$, versus $\log(n)$ at 20% conversion for emulsion polymerization of butadiene at 25°C.

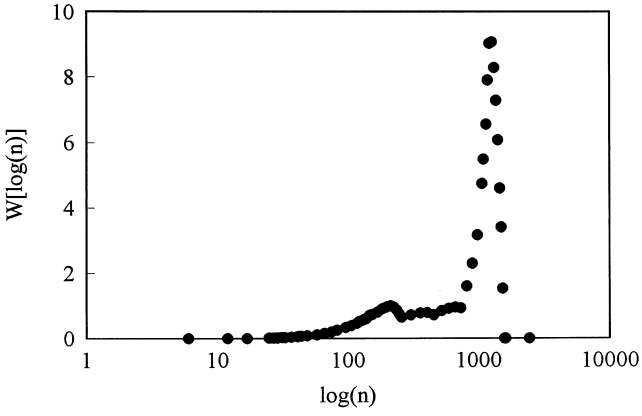

Fig. 5. Simulated weight fraction of logarithm of chain length, $W[\log(n)]$, versus $\log(n)$ at 55% conversion for emulsion polymerization of butadiene at 25°C.

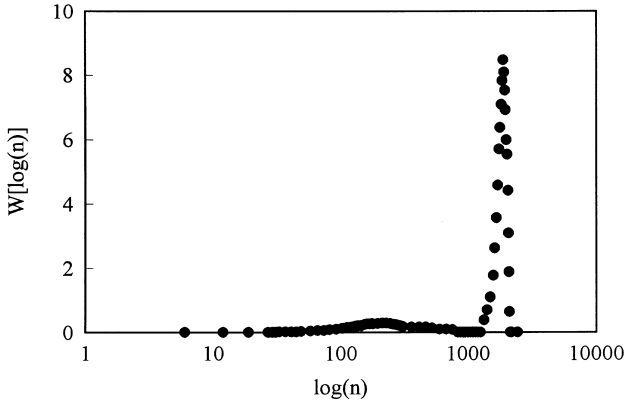

Fig. 6. Simulated weight fraction of logarithm of chain length, $W[\log(n)]$, versus $\log(n)$ at 75% conversion for emulsion polymerization of butadiene at 25°C.

when plotted as $W[\log(n)]$ versus $\log(n)$. Therefore, the chain length distribution became bimodal because of the presence of high extent of tetra-functional crosslinking. This bimodal behavior can be used to advantage in practice to produce polymers with acceptable processability and good mechanical properties. This same effect is observed in emulsion polymerization of styrene–butadiene where the CL4 reaction due to butadiene monomer causes crosslinking and gelation. Furthermore, simulation results indicated that the growth of the second peak in chain length distribution depended strongly on the initiator concentration and the rate of initiation.

In Fig. 7, The chain length corresponding to the maximum of the second peak of the distribution is plotted against conversion. This figure shows that, in the presence of lower molecular weight fraction in the distribution, the maximum chain length of the second fraction increases in a non-linear fashion with conversion. Fig. 8 presents the number and weight fraction of the second peak of the distribution as a function of conversion. According to this figure, the number fraction increases in an approximately linear fashion from zero to 60% as the conversion is increased. On the other hand, the increase in weight fraction with conversion is non-linear and a sharp change in slope of the weight fraction versus conversion is observed between 20 and 40% conversion.

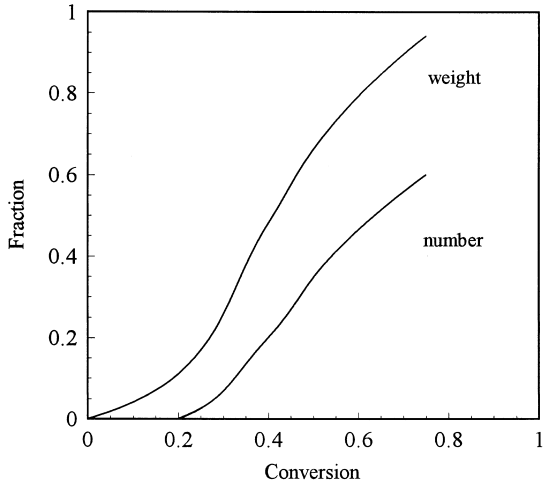

Fig. 8. Simulated weight fraction of the second peak of the bimodal distribution as a function of conversion for emulsion polymerization of butadiene at 25°C.

Fig. 9 shows number (DP_n) and weight (DP_w) average degree of polymerization versus conversion, respectively. The rate of increase of DP_n with conversion was almost constant, therefore the formation of the second peak in the chain length distribution had little effect on DP_n. However, The rate of increase of DP_w with conversion was significantly higher than that of DP_n with conversion. Fig. 10 shows the polydispersity index (PI) as a function of conversion. Before the critical conversion of 20%, the PI was

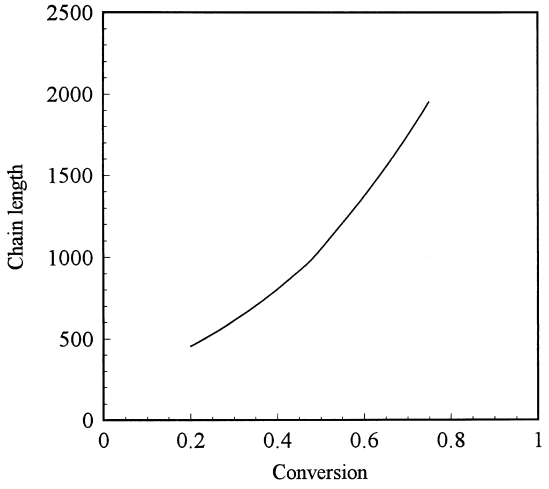

Fig. 7. Simulated chain length corresponding to the maximum of the second peak of the distribution as a function of conversion for emulsion polymerization of butadiene at 25°C.

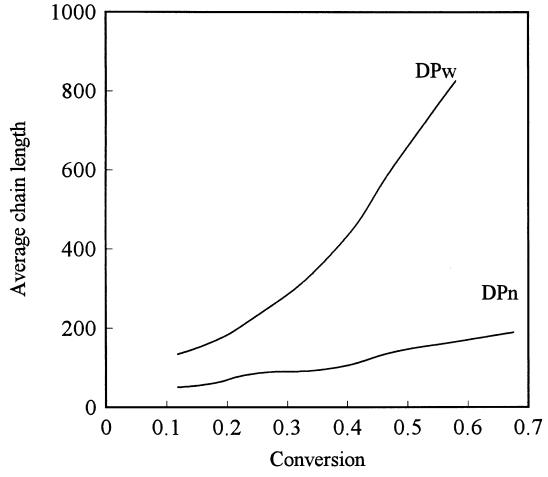

Fig. 9. Simulated number (DP_n) and weight (Dp_w) average degree of polymerization as a function of conversion for emulsion polymerization of butadiene at 25°C.

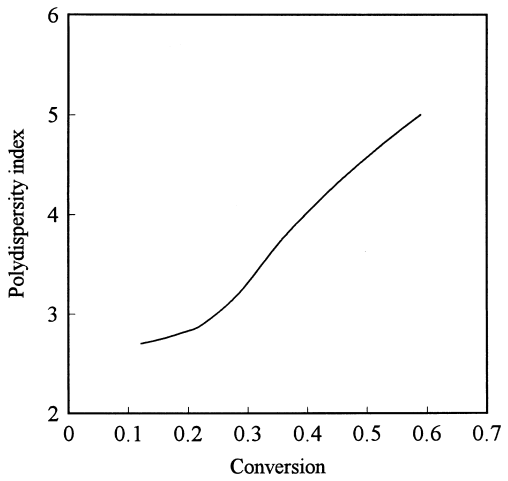

Fig. 10. Polydispersity index as a function of conversion for emulsion polymerization of butadiene at 25°C.

around 3, but above 20% conversion where the effect of tetra-functional crosslinking became significant, PI increased to 5 after 50% conversion. Results of Figs. 9 and 10 indicate that tetra-functional crosslinking has a significant effect on DP_w and PI. However, a sharp change in DP_w is not observed in emulsion polymerization with tetra-functional crosslinking as compared to homogeneous polymerization systems [43].

Tobita and Yamamoto [42] have studied the formation of bimodal molecular weight distribution in emulsion crosslinking coploymerization of vinyl and divinyl monomers using the method of Monte Carlo simulation. Tobia [43] has also studied the formation of bimodal distribution in bulk polymerization systems. According to the simulation results by Tobita and Yamamoto [42] and by Tobita [43], the process of formation of bimodal distribution in emulstion polymerization is quite different from the process for bulk systems. The emulsion polymerization system gives a size dependence because crosslinking between large-sized polymer molecules that exist in different polymer particles are prohibited. Moreover, Tobita and Yamamoto [42] simulated the kinetics of microgel formation in emulsion copolymerization of vinyl and divinyl monomers. They observed that a drastic increase in molecular weights at the gel point that is a characteristic of homogeneous polymerizations is not a requisite for microgel formation and a new definition for gel point may be required in emulsion polymerization.

A microgel is defined as intramolecularly crosslinked macromolecules with sufficiently high molecular weights. In their simulations, Tobita and Yamamoto [42] were able to obtain microgels in emulsion crosslinking coploymerization of vinyl and divinyl monomers by changing the reaction parameters such as the feed ratio and the reactivity ratio of the vinyl and divinyl monomers and the ratio of the rate constant for the crosslinking reaction to the propagation reaction. They further observed that in some cases, depending on reaction parameters, very large polymer molecules that contain many intermolecular crosslinks are formed without the formation of intramolecular crosslinks. Chain length distributions presented in Figs. 3–6 indicate that large intramolecularly crosslinked poymer molecules can be obtained in emulsion polymerization of dienes with high extent of tetra-functional crosslinking. However, we do not have simulation data to show that these intermolecularly crosslinked macromolecules contain high extent of intramolecular crosslinks. Therefore, the formation of microgels in emulsion polymerization of dienes with high extent of tetra-functional crosslinking may be possible but more simulation work is necessary to prove this premise.

4. Conclusions

Direct Monte Carlo simulation was used to study the effect of tri-functional branching and tetra-functional crosslinking on the modality of the chain length distribution in emulsion polymerization of butadiene. The volume of the simulation was 10^5 nm^3, the ratio of monomer to initiator concentration was 500, the ratio of initiator to polymer particle concentration was 2.5 and the number polymer particles were 400. For simulated conversions in the range of 20–75%, a bimodal molecular weight distribution was observed. The maximum of the second peak of the bimodal distribution moved to higher molecular weights as the conversion was increased. As the conversion was increased from 20 to 75%, the increase in the number average molecular weight of the polymer with conversion was linear but a slight increase in the slope of the weight average molecular weight with conversion was observed. More importantly, as the conversion was increased, a significant change in the slope of the weight fraction of the second peak of the molecular weight distribution curve was observed at approximately 20% conversion. Furthermore, results indicate that large intramolecularly crosslinked poymer molecules can be obtained in emulsion polymerization of dienes with high extent of tetra-functional crosslinking. The formation of microgels, defined as intramolecularly crosslinked macromolecules with sufficiently high molecular weights, in emulsion polymerization of dienes with high extent of tetra-functional crosslinking may be possible but more simulation work is necessary to prove this premise.

References

[1] Hamielec AE, MacGregor JF. In: Reichert KH, Geiseler W, editors. Polymer reaction engineering. Munich: Hanser Publishers, 1983 (p. 21).
[2] Polleck M, MacGregor JF, Hamielec AE. ACS Symp Ser 1982;197:209.
[3] Guyot A. In: Reichert KH, Geiseler W, editors. Polymer reaction engineering. Munich: Hanser Publishers, 1983 (p. 287).
[4] Giannetti E. In: Reichert KH, Geiseler W, editors. Polymer reaction engineering. Weinheim: VCH Publishers, 1989 (p. 343).
[5] Cociani M, Canu P, Storti G, Morbidelli M, Carra S. In: Reichert KH,

Geiseler W, editors. Polymer reaction engineering. Weinheim: VCH Publishers, 1989 (p. 199).
[6] Stock JDR. In: Reichert KH, Geiseler W, editors. Polymer reaction engineering. Weinheim: VCH Publishers, 1989 (p. 23).
[7] Harkins WD. J Am Chem Soc 1947;69:1428.
[8] Smith WV, Ewart RH. J Chem Phys 1948;16:592.
[9] Min KW, Ray WH. J Makromol Sci Rev Makromol Chem C 1974;11-2:177.
[10] Katz S, Shinnar R, Saidel GM. Adv Chem Ser 1969;91:145.
[11] Min KW, Ray WH. J Appl Polym Sci 1978;22:89.
[12] Lin CC, Chiu WY. J Appl Polym Sci 1979;23:2049.
[13] Lichti G, Gilbert RG, Napper DH. J Polym Sci Chem Ed 1980;18:1297.
[14] Lichti G, Gilbert RG, Napper DH. In: Piirma I, editor. Emulsion polymerization, New York: Academic Press, 1982 (p. 93).
[15] Gianneti E, Storti G, Morbidelli M. J Polym Sci Polym Chem 1988;26:1835.
[16] Storti G, Polotti G, Cociani M, Morbidelli M. J Polym Sci Polym Chem 1992;30:731.
[17] Sundberg DC, Eliassen JD. In: Fitch IRM, editor. Polymer colloids, New York: Plenum Press, 1971 (p. 153).
[18] Friis N, Hamielec AE. J Appl Polym Sci 1975;19:97.
[19] Bamford CH, Tompa H. J Polym Sci 1953;10:345.
[20] Bamford CH, Tompa H. Trans Faraday Soc 1954;50:1097.
[21] Bamford CH, Barb WG, Jenkins AD, Onyon PF. Kinetics of vinyl polymerization by free radical mechanism. London: Butterworth, 1958 (chap. 7).
[22] Nagasubramanian K, Graessley WW. Chem Engng Sci 1970;25:1559.
[23] Nagasubramanian K, Graessley WW. Chem Engng Sci 1970;25:1549.
[24] Chatterjee A, Kabra K, Graessley WW. J Appl Polym Sci 1977;21:1751.
[25] Chetterjee A, Park WS, Graessley WW. Chem Engng Sci 1977;32:167.
[26] Villermaux J, Blavier L. Chem Engng Sci 1984;39-1:87.
[27] Villermaux J, Blavier L. Chem Engng Sci 1984;39-1:101.
[28] Taylor TW, Reichert KH. J Appl Polym Sci 1985;30:227.
[29] Tobita H, Hamielec AE. Makromol Chem Macromol Symp 1988;20:501.
[30] Tobita H, Hamielec AE. Macromolecules 1989;22:3098.
[31] Tobita H, Hamielec AE. In: Reichert KH, Geiseler W, editors. Polymer reaction engineering. Weinheim: VCH Publishers, 1989 (p. 43).
[32] Kuchanov SI, Pismen LM. Polym Sci USSR 1971;13:2288.
[33] Tobita H. Polym React Engng 1993;1:379.
[34] Tobita H. J Polym Sci: Polym Phys Ed 1993;31:1363.
[35] Tobita H. Macromolecules 1993;26:836.
[36] Tobita H. Makromol Chem Theory Simul 1993;2:761.
[37] Tobita H. Macromolecules 1993;26:5427.
[38] Tobita H. Macromolecules 1992;25:2671.
[39] Tobita H. Polym React Engng 1993;1:357.
[40] Tobita H, Kimura K, Fugita K, Nomura M. Polymer 1993;4:2569.
[41] Tobita H. Polymer 1994;35:3023.
[42] Tobita H, Yamamoto K. Macromolecules 1994;27:3389.
[43] Tobita H. Macromol Theory Simul 1998;7:225.
[44] Sadhir RK, Luck RM. Expanding monomers. Synthesis, characterization, and application. Boca Raton, FL: CRC Press, 1992 (p. 83).
[45] Flory PJ. Principles of polymer chemistry. Ithaca, NY: Cornell University Press, 1953 (p. 158).
[46] Odian G. Principles of polymerization. 2nd ed. New York: Wiley, 1970 (p. 258).
[47] Brandrup J, Emmergut EH. Polymer handbook. 3rd ed. New York: Wiley, 1989 (pp. II-68, II-83, II-87).
[48] Tate DP, Bethea TW. In: Kroschwitz JI, editor. Encyclopedia of polymer science and engineering, vol. 2. New York: Wiley, 1985 (p. 540, 574).
[49] Friedman EM. Polym Engng Sci 1990;30-10:569.